Controlled tunneling-induced dephasing of Rabi rotations for high-fidelity hole spin initialization

P.-L. Ardelt,[1] T. Simmet,[1] K. Müller,[2] C. Dory,[1,2] K. A. Fischer,[2] A. Bechtold,[1] A. Kleinkauf,[1,2] H. Riedl,[1] and J. J. Finley[1,*]

[1]*Walter Schottky Institut and Physik-Department, Technische Universität München, Am Coulombwall 4, 85748 Garching, Germany*

[2]*E. L. Ginzton Laboratory, Stanford University, Stanford, California 94305, USA*

We report the subpicosecond initialization of a single heavy hole spin in a self-assembled quantum dot with >98.5% fidelity and *without* external magnetic field. Using an optically addressable charge and spin storage device we tailor the relative electron and hole tunneling escape time scales from the dot and simultaneously achieve high-fidelity initialization, long hole storage times, and high-efficiency readout via a photocurrent signal. We measure electric-field-dependent Rabi oscillations of the neutral and charged exciton transitions in the ultrafast tunneling regime and demonstrate that tunneling-induced dephasing (TID) of excitonic Rabi rotations is the major source for the intensity damping of Rabi oscillations in the low Rabi frequency, low temperature regime. Our results are in very good quantitative agreement with quantum-optical simulations revealing that TID can be used to precisely measure tunneling escape times and extract changes in the Coulomb binding energies for different charge configurations of the quantum dot. Finally, we demonstrate that for subpicosecond electron tunneling escape, TID of a coherently driven exciton transition facilitates ultrafast hole spin initialization with near-unity fidelity.

I. INTRODUCTION

The spin degree of freedom of charge carriers in semiconductor nanostructures is promising for the realization of quantum information technologies [1,2]. In particular, spins locally trapped in optically active semiconductor quantum dots (QDs) have recently attracted strong interest, since their efficient coupling to light enables ultrafast spin control [3–6], single-shot readout of spin states [7,8] and, more recently, the entanglement of stationary spins and photons [9–11] as the first building block for the realization of a quantum repeater [12]. For all associated quantum protocols the high-fidelity initialization of single spin states that can be generated on-demand on ultrashort time scales [13–15] and the reliable storage of the spin state are crucial [16,17]. The initialization of single spins can either be performed by spin-pumping of a charged QD [14] or by tunneling ionization of photogenerated excitons [13,18–21]. While spin pumping is very convenient since it requires only a single continuous wave laser, it is rather slow with reported initialization fidelities of >90% after ∼1 ns. On the other hand, tunneling ionization of photogenerated excitons without magnetic fields has been achieved with >96% preparation fidelities over picosecond time scales by exploiting ultrafast intramolecular tunneling in quantum dot molecules [13] or shallow QDs [21]. In both cases, the high fidelity is only achieved for specific experimental conditions that limit the hole lifetime. Moreover, the experiments presented in Ref. [21] were performed with continuous wave excitation that is unsuitable for highly precise on-demand generation of hole spin qubits and allows the dynamics of the system only to be inferred with indirect techniques such as linewidth broadening [22] due to the incoherent nature of the continuous wave–quantum dot interaction.

Here, we demonstrate the spin initialization of a single heavy hole spin with a preparation fidelity >98.5%

on subpicosecond time scales *without* applying a magnetic field. The heavy hole spin is initialized by partial tunneling ionization of excitons prepared using ultrafast optical methods in an InGaAs QD embedded in a Schottky diode structure [13,23]. In order to maximize the spin initialization fidelity, (i) we engineer the band structure to tailor the electron and hole tunneling times from the QD by optimizing the Al content in an AlGaAs blocking barrier adjacent to the QD and (ii) we operate the Schottky diode structure in the ultrafast tunneling regime, where electron tunneling occurs on time scales similar to the pulsed coherent excitation of an exciton. Accordingly, we experimentally record and theoretically model an intensity damping of excitonic Rabi oscillations due to tunneling-induced dephasing (TID). By investigating electron tunneling from a charged exciton state, we demonstrate that TID can vice versa be used to determine electron tunneling times on time scales difficult to access by conventional pump-probe spectroscopy. Finally, we show that in the TID regime a single heavy hole spin can be initialized with fidelities exceeding >98.5%, overcoming prior limitations of the spin initialization fidelity due to the fine structure precession of the electron-hole pairs prior to ionization and making the initialization insensitive to errors in the excitation pulse intensity.

II. EXPERIMENTAL METHODS

The sample consists of a single layer of self-assembled InGaAs QDs embedded in an n-i Schottky diode [24]. The QDs are placed 125nm above a heavily n-doped back contact and covered with a further 125 nm thick layer of GaAs. For hole storage samples, we integrate an additional 20 nm think $Al_{0.1}Ga_{0.9}As$ barrier 10 nm above the QDs into the GaAs layer as schematically illustrated in the rightmost panel of Figs. 2(a) and 2(b). The Schottky diode is formed by a 3 nm semitransparent Ti layer covered with a shadow mask of Au with circular 1–2 μm diameter apertures to ensure that we optically address only single QDs [25]. Most importantly,

*finley@wsi.tum.de
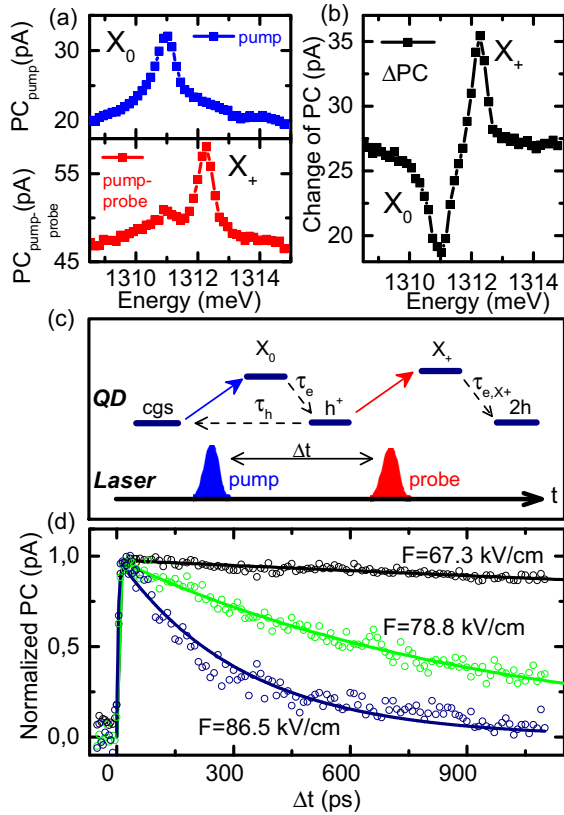
FIG. 1. (Color online) (a) PC absorption spectra for one (blue) and two pulse (red) excitation probing absorption of the neutral exciton transition X_0 and positive trion transition X_+, respectively. (b) Difference of PC spectra $\Delta\mathrm{PC} = \mathrm{PC}_{\mathrm{pump-probe}} - \mathrm{PC}_{\mathrm{pump}}$ for one and two pulse excitation. (c) Schematic illustration of the charge carrier dynamics probed in (b): The second excitation pulse at a delay time Δt probes the positive trion X_+ as the electron tunnels out of the QD faster than the hole $\tau_e \ll \tau_h$. (d) PC amplitude of the trion transition X_+ as a function of the probe-pulse delay Δt. With increasing field the tunneling rate of the hole increases. Fits using a rate equation model are presented as solid lines.

applying a bias between the Au top contact and the n-doped back contact facilitates control of the local electric field F in the growth direction at the QDs and thus control of the electron and hole tunneling times τ_e and τ_{hh} from the QDs. For τ_e shorter than the radiative recombination time $\tau_{\mathrm{rad}} > \tau_e$ of the electron-hole pairs, the Schottky diode structure is operated in the photocurrent (PC) regime. There, resonant absorption of the excitation laser leads to a measurable change of current in the external measurement circuit [26].

Typical raw data obtained in such a PC experiment are presented in Fig. 1(a). The figure shows the PC induced in the sample when exciting a single QD in the PC regime with a train of 5 ps laser pulses (pump) including a PC background resulting from the dark current across the diode and absorption of scattered light in the QD layer [27]. To achieve continuous tuning of the laser wavelength the pulses are derived from a 150 fs broadband Ti:sapphire laser source (repetition rate 79 MHz) by using a 4f-pulse-shaping geometry [3,19,28]. A clear peak is observed at $E = 1311.0$ meV arising from resonantly driving the neutral exciton transition X_0 in the

QD. In order to investigate the dynamics of charge carriers excited by the pump-pulse train, we add a second train of laser pulses delayed by a time Δt as schematically illustrated in Fig. 1(c). A typical PC-absorption spectrum for two-pulse excitation with the first pulse fixed to the crystal ground state (cgs) $\to X_0$ transition and the second pulse (probe), delayed by $\Delta t = 25$ ps and tunable in energy, is presented in Fig. 1(a) in red. Comparing the one and two pulse PC absorption spectra in Fig. 1(a) shows that the amplitude of the neutral exciton transition X_0 is strongly suppressed, while an additional peak emerges at $E = 1312.3$ meV, detuned by 1.3 meV from the neutral exciton transition. This additional peak results from the single hole h^+ to positively charged trion transition X_+ as will be discussed below. The change of the absorption spectrum becomes even clearer by plotting the change of PC, namely $\Delta\mathrm{PC} = \mathrm{PC}_{\mathrm{pump-probe}} - \mathrm{PC}_{\mathrm{pump}}$ as presented in Fig. 1(b). Dips correspond to PC absorption for excitation with a single laser pulse (pump) and peaks to conditional PC absorption for excitation with a second laser pulse (probe).

The conditional bleaching of the X_0 amplitude and emergence of the X_+ absorption by a second excitation pulse can be understood from the dynamics illustrated in Fig. 1(c): The population of the QD, initially in the crystal ground state cgs, is transferred to the neutral exciton cgs $\to X_0$ with a Rabi rotation around π by the pump-pulse [blue arrow in Fig. 1(c)] and decays by subsequent tunneling of the electron and the heavy hole. This occurs with characteristic time scales τ_e for the electron tunneling $X_0 \dashrightarrow h^+$ and τ_h for the hole tunneling $h^+ \dashrightarrow$ cgs back to the cgs [19,29], where dashed arrows indicate transitions due to tunneling in contrast to full arrows indicating optically driven transitions. Primarily due to the lighter electron effective mass of $m_e^* = 0.05 m_0$ compared to the hole $m_{hh}^* = 0.34 m_0$ (m_0 denotes the free electron mass) [31], the electron tunneling time is typically shorter than the heavy hole hole tunneling time $\tau_e < \tau_h$ [13]. When the second pulse arrives with a time delay $\tau_e < \Delta t < \tau_h$, the neutral exciton transition cgs $\to X_0$ cannot be driven as the QD is occupied with a single hole h^+. However, the probe pulse can excite the single hole to positive trion transition $h^+ \to X_+$, that is positively detuned by an energy $\Delta E = 1.3$ meV from the neutral exciton X_0 [cf. red arrow in Fig. 1(c)]. The difference in energy results from the Coulomb and exchange interaction with the additional hole h^+. Thus, monitoring the amplitude of the X_+ transition as a function of the probe laser delay Δt allows us to extract (i) the electron tunneling time τ_e from the rise time of the X_+ amplitude as electron tunneling from the neutral exciton state X_0 enables the $h^+ \to X_+$ transition and (ii) the heavy hole tunneling time τ_h from the decay time of the X_+ amplitude.

In Fig. 1(d), we present the time evolution of the amplitude of the trion transition $h^+ \to X_+$ as a function of the time delay Δt between the pump and probe pulse at three different electric fields F. The amplitude of the X_+ transition in Fig. 1(d) rises immediately corresponding to a very fast electron tunneling time ($\tau_e < 5$) ps. The decay time due to hole tunneling is much longer and decreases from $\tau_h = 9.8$ ns to $\tau_h = 322$ ps when increasing the internal electric field across the Schottky diode from $F = 67.3$ kV/cm up to $F = 86.5$ kV/cm. Note, however, that quantitative access to the electron tunneling times $\tau_e < \tau_{\mathrm{pulse}} = 5$ ps is impossible, since the time resolution of
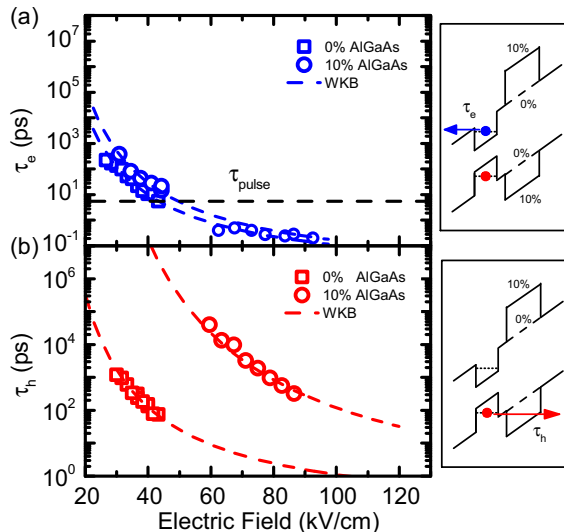
FIG. 2. (Color online) Comparison of the field-dependent tunneling times for two samples with and without the 10% AlGaAs barrier. (a) Electric-field-dependent electron and (b) hole tunneling times. Fits to the data using the WKB model are plotted as dashed lines.

pump-probe experiments is inherently limited by the pulse length τ_{pulse}. In order to extract the tunneling times τ_e and τ_h, we model the time evolution of the X_+ transition amplitude with a rate equation model incorporating the populations of neutral exciton X_0, the positively charged trion X_+, and the crystal ground state cgs [29] (see Supplemental Material [30]).

III. OPTIMIZED SPIN STORAGE DEVICE FOR PHOTOCURRENT READOUT

In order to use the Schottky diode structure as a spin storage device, independent engineering of the tunneling times τ_e and τ_h is crucial. Ideally, for a hole spin storage device, we aim for two properties: (i) An ultrafast electron tunneling time τ_e, since the electron tunneling time τ_e determines the time scale on which a single hole spin can be initialized by tunneling ionization of the neutral exciton X_0, and (ii) a long hole storage time τ_h that facilitates use of the hole spin qubit. The individual tunneling times τ_e and τ_h can be tailored by incorporating an $Al_xGa_{1-x}As$ barrier immediately adjacent to the QD layer [17]. As schematically illustrated in Figs. 2(a) and 2(b) for a heavy hole tunneling barrier, the charge carrier tunneling out of the QD faces an additional barrier with a height that depends on the Al concentration x of the barrier allowing one to design the asymmetry of the tunneling times *a priori* using WKB theory [32,33].

In Figs. 2(a) and 2(b), we present the electron and hole tunneling times τ_e and τ_h for two devices: One n-i Schottky diode with 125 nm GaAs below and above the QD layer, respectively (results shown as squares), and a second diode, where a 20 nm thick tunneling barrier with 10% Al concentration was inserted 10 nm above the QD layer (results shown as circles). To be able to compare the tunneling times, the two QDs compared have similar transition energies of the neutral exciton X_0.

The electron tunneling times τ_e presented in Fig. 2(a) extracted from the rise time of the X_+ amplitude and continuous wave PC measurements of the linewidth of X_0 (see Supplementary Material [30]) exhibit a similar electric field dependence, demonstrating that electron tunneling is not affected by barriers above the QDs. In contrast, the heavy hole tunneling time τ_h in Fig. 2(b) exhibits an approximately three orders of magnitude increase due to the $Al_{0.1}Ga_{0.9}As$ barrier. To quantitatively analyze the data we calculate the tunneling times using a WKB model [32,33]:

$$\tau_{e(h)}(F) = \frac{2m^*_{e(h)}L^2}{\hbar\pi} \exp\left[\frac{4}{3\hbar eF}\sqrt{2m^*_{e(h)}E_i^3}\right], \quad (1)$$

where $m^*_{e(h)}$ denotes the effective mass of electrons (heavy holes), L the effective width of the QD potential in the z direction, F the electric field, and E_i the height of the triangular barrier in the conduction (valence) band. Fits to the data are presented as dashed lines and produce good overall agreement with our experimental data.

Modeling the effect of the $Al_{0.1}Ga_{0.9}As$ barrier on the hole tunneling time, we obtain an effective mass of $m^*_h = 0.34m_0$ for the heavy holes and an effective width for the QD potential of $L = 5.1$ nm [29], when increasing the height of the triangular barrier in the valence band from $E_{i,0\%} = 39.8$ meV to $E_{i,10\%} = 73.0$ meV. The increase of the triangular barrier height $\Delta E_i = 33.2$ meV qualitatively agrees with the valence band offset $\Delta E_v = 40$ meV due the 10% Al concentration in the barrier, while the effective width L and effective mass are in good agreement with previously reported values for quantum dots with a similar material composition [29].

IV. TUNNELING-INDUCED DEPHASING OF RABI ROTATIONS

To minimize the hole spin initialization time, we operate the Schottky diode in the electric field regime $F > 50$ kV/cm, where the electron tunneling time τ_e corresponding to the ionization time of the neutral exciton X_0 is shorter than the pulse length of the excitation laser τ_{pulse}. However, when the interaction time between QD and laser becomes comparable to the lifetime of the driven state (which is given by τ_e), this can no longer be neglected as a source of dephasing [33,34]. The blue data points in Fig. 3(a) show the photocurrent as a function of the pulse area Ω of the driving laser in resonance with the neutral exciton X_0 and electric fields in the range $F = 59.6$ kV/cm to $F = 71.2$ kV/cm (where a linearly increasing background determined with an off-resonant laser pulse has been subtracted) [27]; an electric field region where the electron tunneling time τ_e is clearly shorter than the excitation laser pulse lengths of $\tau_{\text{pulse}} \cong 5$ ps. While for an electric field of $F = 59.6$ kV/cm in Fig. 3(a) a damped 2π Rabi rotation indicated by the black arrow can still be resolved [34,35], increasing the electric field to 71.2 kV/cm leads to a complete dephasing of the Rabi rotations. Importantly, the current does not converge towards a value that is lower than the maxima of the oscillations but instead converges towards the maximum given by the repetition rate of the laser corresponding to a PC of 12.8 pA for a repetition rate of 79 MHz.

We continue to show that the damping of the observed Rabi oscillations in Fig. 3(a), as well as convergence to the
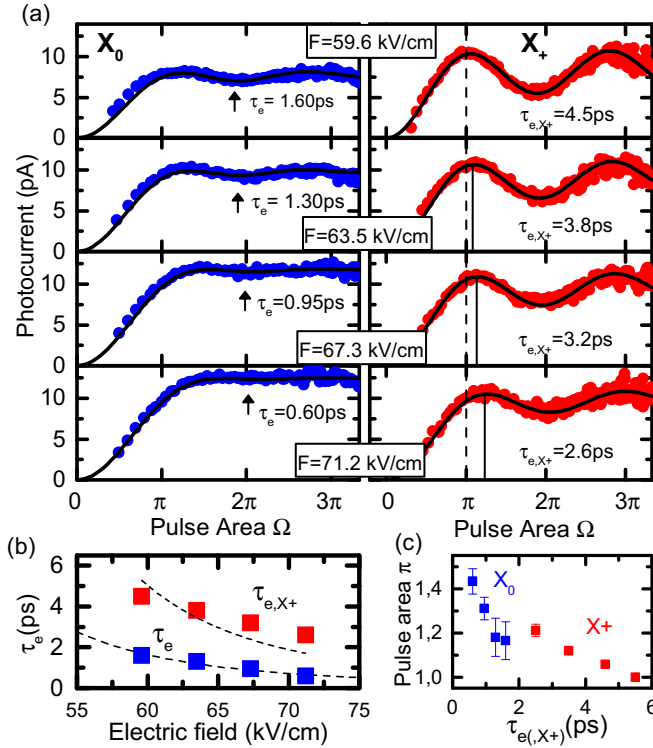
FIG. 3. (Color online) (a) Damped Rabi rotations of the neutral X_0 and charged exciton X_+. Increasing the electric field leads to faster electron tunneling τ_e and τ_{e,X_+} and stronger TID. (b) Electron tunneling times extracted from modeling the TID for the neutral τ_e and charged τ_{e,X_+} exciton. (c) Renormalization of the area of a π pulse due to increased dephasing of the Rabi rotations.

maximum value, results exclusively from the fast electron tunneling. Typically the dephasing of excitonic Rabi rotations is induced by the high-power density pulse of the excitation via the coupling to LA phonons. The dephasing induced by the excitation results in an intensity damping of the Rabi oscillations with an increasing Rabi frequency of the excitation pulse [34,35]. However, as we operate the QD at a low temperature of $T = 4.2$ K and for pulse areas up to 3π, corresponding to the low Rabi frequency limit [36], the corresponding excitation-induced dephasing time (that scales linearly with squared Rabi frequency of the excitation) laser is weak. Comparing the electron tunneling rates $(t_e)^{-1}$ and $(t_{e,X+})^{-1}$ with a lower boundary of the dephasing rate $\Gamma_{\text{phonons}} = (35.3 \text{ ps})^{-1}$ induced by the excitation [37] clearly identifies TID as the major source of dephasing for the neutral exciton Rabi rotations presented in Fig. 3(a). To model the resulting damping of the Rabi rotations in Fig. 3(a) in the TID regime quantitatively, we performed quantum optical simulations using the Quantum Optical Toolbox in Python (QUTIP) [38]. We utilized the Lindblad form of the quantum optical master equation to simulate Rabi oscillations of the charge carrier dynamics described in Fig. 1(c). TID was taken as a phenomenological dephasing rate and was extracted at different field strength through fits to the experimental data in Fig. 3(a). Due to the extremely long hole tunneling time and high fidelity of initialization, each simulation was reduced to a three-level subsystem. The result of these simulations is presented as black lines on top of the data in Fig. 3(a) and

produces excellent agreement. The tunneling times extracted from the simulations are presented in Fig. 3(b) as blue data points and range from $\tau_e = 1.60$ ps at $F = 59.6$ kV/cm to $\tau_e = 0.60$ ps at $F = 71.2$ kV/cm. The WKB fit from Fig. 2(a) is reproduced in this figure as well and produces very good quantitative agreement.

We proceed by utilizing the TID of the Rabi rotations to precisely measure the electron tunneling times τ_{e,X_+} from the positively charged trion state X_+ [schematically shown in Fig. 1(c)]. Therefore, we present the Rabi rotations of the positively charged exciton state X_+ as a function of pulse area of the probe pulse in red in Fig. 3(a). Similar to the neutral exciton X_0, the intensity of the Rabi oscillations is progressively damped when increasing the electric field from $F = 59.6$ kV/cm to $F = 71.2$ kV/cm. However, comparing the damping of the neutral exciton X_0 and charged state X_+ Rabi oscillations in Fig. 3(a), we clearly observe a stronger TID for the neutral exciton X_0. This indicates that electron tunneling from X_+ occurs significantly more slowly than from X_0. In order to extract these electron tunneling times τ_{e,X_+} from the charged exciton state X_+, we fit the data with the model described above. The fits are presented as black lines on top of the experimental data in Fig. 3(a) and produce excellent agreement, as for the neutral exciton X_0.

The extracted tunneling times from the charged exciton X_+ state are presented in Fig. 3(b) as red data points. Comparing them to the values obtained for electron tunneling from X_0 [Fig. 3(b), blue] shows that for the same electric field tunneling from X_+ occurs significantly more slowly than from X_0. The increased electron tunneling times τ_{e,X_+} from the charged exciton state X_+ can be understood in the following way: For tunneling from the charged state $X_+ \dashrightarrow 2h$ illustrated in Fig. 1(b) an additional Coulomb attraction from the second heavy hole in the QD has to be overcome by the electron. We calculate the additional Coulomb attraction by fitting the electron tunneling times τ_{e,X_+} presented in Fig. 3(b) with a WKB fit where the barrier height E_i, corresponding to an additional ionization energy here is varied while all other parameters are kept from the fit presented above [Fig. 2(a)]. This results in an additional ionization energy $\Delta E_i = 11.2$ meV which is in agreement with prior calculations of the additional exciton binding energy of second heavy hole $2h$ present in the QD including spatial rearrangement of the electron and hole wave functions [39]. Note that due to the spatial rearrangement of the strongly localized hole wave functions in the QD, the energy reduction due the Coulomb attraction between $1e$ and the second heavy hole $2h$ exceeds the energy increase due to the Coulomb repulsion between the two heavy holes $2h$ leading to the observed increase in ionization energy ΔE_i.

Closer inspection of Fig. 3(a) also reveals that the maxima of the oscillations shift to higher powers for larger electric fields as indicated for the shift of the position of a π pulse for the charged exciton X_+. To analyze this in more detail, we present in Fig. 3(c) the pulse area of a renormalized π pulse for the X_0 and the X_+ transitions as a function of the tunneling times τ_e and τ_{e,X_+}, respectively. The reduction of the Rabi frequency results from a renormalization due to dephasing, similar to renormalization resulting from strong dephasing due to LA phonons at elevated temperatures [36].
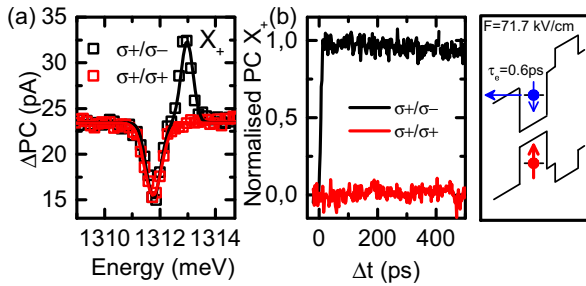
FIG. 4. (Color online) (a) Co- and cross-circularly polarized pump-probe measurements of the trion transition X_+. The complete suppression of the trion amplitude X_+ for a co-polarized excitation due to the Pauli blockade demonstrates high-fidelity spin initialization. (b) Time evolution of the X_+ amplitudes from (a) and a schematic illustration of the hole spin initialization due to electron tunneling ionization. The rise time corresponds to the spin initialization time. The suppression of the $h^+ \rightarrow X_+$ transition amplitude driven with σ_+/σ_+ polarized light indicates high-fidelity spin initialization and storage.

V. SUBPICOSECOND HIGH-FIDELITY HOLE SPIN INITIALIZATION

Finally, we demonstrate high-fidelity hole spin initialization in the TID regime $\tau_e < \tau_{\text{pulse}}$. Thereby, we excite the QD with σ_+ polarized excitation pulse to create a neutral exciton X_0 with a spin configuration $\downarrow\Uparrow$, as illustrated schematically in Fig. 4. The exciton spin state coherently precesses due to the e-h exchange interaction with a period of 78 ps between $\downarrow\Uparrow$ and $\uparrow\Downarrow$ [3] (see Supplemental Material [30]). However, if the exciton X_0 is ionized by electron tunneling on time scales of $\tau_e \ll 78$ ps, the remaining hole in the QD has a very well defined spin $\Uparrow$ projection parallel to the initially generated exciton $\downarrow\Uparrow$, defined by the optical axis and circular polarization of the excitation source. The fidelity of the hole spin $\Uparrow$ initialization thus depends on τ_e, since any precession of the spin wave function prior to the tunneling ionization will result in a statistical mixture of $\Uparrow$ and $\Downarrow$ for the hole spin [13,19,23]. Note here that the TID makes the spin preparation insensitive to errors in the intensity of the excitation pulse as can be seen in Fig. 3(a) while the increasing PC with decreasing tunneling time τ_e indicates a high success rate for the spin initialization.

To investigate the spin initialization fidelity in the regime $\tau_{\text{pulse}} > \tau_e$, we performed cross- and co-circularly polarized pump-probe measurements on the positively charged trion transition X_+. A typical spectrum recorded at an electric field $F = 71.7$ kV/cm is shown in Fig. 4(a). While for the cross-polarized PC trace (σ_+/σ_-) in black a clear peak from the X_+ transition is resolved, for the co-polarized PC trace (σ_+/σ_-) the amplitude of the X_+ transition in Fig. 4(a) is completely suppressed due to Pauli blocking [13]. We estimate the initialization fidelity of the heavy hole spin to be $F_\Uparrow > 98.5\%$ using Gaussian fits of the PC absorption peaks with height A of the positive trion X_+ for co- and cross-polarized excitation presented in Fig. 4(a) and define the hole spin initialization fidelity as $F_\Uparrow = 1 - \frac{A_{\sigma_+/\sigma_+}}{A_{\sigma_+/\sigma_+}+A_{\sigma_+/\sigma_-}}$ [19,23]. Note that the fidelity of the hole spin is mainly limited

by the accuracy of fitting the area and the measurement noise and thus we only give a lower bound for $F_\Uparrow$. Since the projection of the heavy hole spin on the z axis scales with the cosine of the exchange interaction precession angle, the initialization fidelity for spin initialization times $\tau_e = 0.6$ ps is expected to exceed $F_\Uparrow > 98.5\%$.

To demonstrate that the hole spin state $\Uparrow$ is stored with high fidelities, we present in Fig. 4(b) the time dependence of the positively charged trion X_+ at $F = 71.7$ kV/cm for time delays between $\Delta t = 0$ ns and $\Delta t = 0.5$ ns. The rise time τ_e of the cross-polarized amplitude encoded in black in Fig. 4(b) directly corresponds to the heavy hole spin initialization time and confirms the ultrafast initialization of the spin state $\Uparrow$. The constant suppression of the amplitude of the X_+ initialized and probed with σ_+/σ_+ polarized light presented in red in Fig. 4(b) confirms that the heavy hole spin $\Uparrow$ is stored with a very high fidelity over the entire time range probed. Note that by locking the excitation laser pulse to an electric field modulation, the Schottky diode structure can be switched to low electric field values after the heavy hole spin initialization allowing for storage times extending into the μs range for electric fields below ~ 50 kV/cm. For the current device, an electric field modulation of $\Delta F = 40.5$ kV/cm can easily be synchronized with the laser pulse excitation (see Supplemental Material [30]). Using an RC circuit model, we measure a response time of the diode to the electrical field modulations of $\tau_{RC} = 1.82$ ns, which is still smaller than the hole storage time (e.g., $\tau_h = 2.8 \pm 0.3$ ns at the electric field of $F = 71.7$ kV/cm in Fig. 4). This makes the diode structure suitable for electrical switching schemes with increasing complexity; e.g., spin initialization is performed at an electric field F_1 and storage (and/or control in Voigt geometry) at an electric field F_2.

VI. CONCLUSION

In summary, we demonstrated the *subpicosecond* initialization of a single heavy hole spin without the need for a supporting external magnetic field with a fidelity of $F_\Uparrow > 98.5\%$. Thereby, the heavy hole spin was initialized by tunneling ionization of a coherently driven neutral exciton X_0. Using an $Al_{0.1}Ga_{0.9}As$ barrier adjacent to the QD we separately control tunneling times of holes and electrons for (i) subpicosecond hole spin initialization and (ii) simultaneous high-efficiency photocurrent readout of the QD charge and spin state. Embedding the QD layer in a Schottky diode structure allows for additional tuning of the charge carrier tunneling times by changing the applied electric field in the growth direction. By mapping out field-dependent Rabi oscillations of the neutral X_0 and positively charged exciton X_+ transitions, we identified tunneling-induced dephasing of Rabi rotations as the major source for a strong intensity damping in this regime. Quantum optical simulations are in excellent agreement with the measurements and revealed that tunneling-induced dephasing of Rabi oscillations can be used to extract the electron tunneling times from the excited state. This allowed inferring the change of Coulomb binding energy for having two holes in the QD. Most strikingly, strong tunneling-induced dephasing of a neutral exciton

transition results in the high-fidelity initialization of single hole states that is insensitive to errors in the excitation pulse intensity. In polarization-resolved pump-probe measurements we demonstrated subpicosecond hole spin initialization with near-unity fidelity and long hole storage times.

The very fast and high fidelity initialization of single heavy hole spins makes the presented device structure an ideal candidate for the realization of qubits and quantum protocols requiring high-fidelity gate operations, especially an ultrahigh-fidelity qubit initialization that works on-demand in Voigt geometry [12]. Furthermore, the presented device and spin initialization enables the possibility to investigate hole spin dynamics at zero magnetic fields over increasing time ranges that are governed by the complex spin-bath interactions as have only recently been measured for electrons [40].

Note added in proof. Recently, we became aware of reference [41] reporting similar ultra-high initialization fidelities for single heavy hole spins by tuning the fine-structure of the ionized neutral exciton X_0 using the optical Stark effect.

[1] D. Loss and D. P. DiVincenzo, Phys. Rev. A **57**, 120 (1998).

[2] B. E. Kane, Nature (London) **393**, 133 (1998).

[3] K. Müller, T. Kaldewey, R. Ripszam, J. S. Wildmann, A. Bechtold, M. Bichler, G. Koblmüller, G. Abstreiter, and J. J. Finley, Sci. Rep. **3**, 1906 (2013).

[4] D. Press, T. D. Ladd, B. Zhang, and Y. Yamamoto, Nature (London) **456**, 218 (2008).

[5] D. Press, K. De Greve, P. L. McMahon, T. D. Ladd, B. Friess, C. Schneider, M. Kamp, S. Höfling, A. Forchel, and Y. Yamamoto, Nat. Photonics **4**, 367 (2010).

[6] K. De Greve, P. L. McMahon, D. Press, T. D. Ladd, D. Bisping, C. Schneider, M. Kamp, L. Worschech, S. Höfling, A. Forchel, and Y. Yamamoto, Nat. Phys. **7**, 872 (2011).

[7] A. N. Vamivakas, C. Y. Lu, C. Matthiesen, Y. Zhao, S. Fält, A. Badolato, and M. Atatüre, Nature (London) **467**, 297 (2010).

[8] A. Delteil, W. B. Gao, P. Fallahi, J. Miguel-Sanchez, and A. Imamoğlu, Phys. Rev. Lett. **112**, 116802 (2014).

[9] K. De Greve, L. Yu, P. L. McMahon, J. S. Pelc, C. M. Natarajan, N. Y. Kim, E. Abe, S. Maier, C. Schneider, M. Kamp, S. Höfling, H. H. Hadfield, A. Forchel, M. M. Fejer, and Y. Yamamoto, Nature (London) **491**, 421 (2012).

[10] W. B. Gao, P. Fallahi, E. Togan, J. Miguel-Sanchez, and A. Imamoglu, Nature (London) **491**, 426 (2012).

[11] J. R. Schaibley, A. P. Burgers, G. A. McCracken, L. M. Duan, P. R. Berman, D. G. Steel, A. S. Bracker, D. Gammon, and L. J. Sham, Phys. Rev. Lett. **110**, 167401 (2013).

[12] P. L. McMahon and K. De Greve, arXiv:1501.03535.

[13] K. Müller, A. Bechtold, C. Ruppert, C. Hautmann, J. S. Wildmann, T. Kaldewey, M. Bichler, H. J. Krenner, G. Abstreiter, M. Betz, and J. J. Finley, Phys. Rev. B **85**, 241306 (2012).

[14] M. Atatüre, J. Dreiser, A. Badolato, A. Högele, K. Karrai, and A. Imamoglu, Science **312**, 551 (2006).

[15] B. D. Gerardot, D. Brunner, P. A. Dalgarno, P. Öhberg, S. Seidl, M. Kroner, K. Karrai, N. G. Stoltz, P. M. Petroff, and R. J. Warburton, Nature (London) **451**, 441 (2008).

[16] M. Kroutvar, Y. Ducommun, D. Heiss, M. Bichler, D. Schuh, G. Abstreiter, and J. J. Finley, Nature (London) **432**, 81 (2004).

[17] D. Heiss, V. Jovanov, M. Caesar, M. Bichler, G. Abstreiter, and J. J. Finley, Appl. Phys. Lett. **94**, 072108 (2009).

[18] A. J. Ramsay, S. J. Boyle, R. S. Kolodka, J. B. B. Oliveira, J. Skiba-Szymanska, H. Y. Liu, M. Hopkinson, A. M. Fox, and M. S. Skolnick, Phys. Rev. Lett. **100**, 197401 (2008).

[19] T. M. Godden, J. H. Quilter, A. J. Ramsay, Y. Wu, P. Brereton, S. J. Boyle, I. J. Luxmoore, J. Puebla-Nunez, A. M. Fox, and M. S. Skolnick, Phys. Rev. Lett. **108**, 017402 (2012).

[20] T. M. Godden, J. H. Quilter, A. J. Ramsay, Y. Wu, P. Brereton, I. J. Luxmoore, J. Puebla, A. M. Fox, and M. S. Skolnick, Phys. Rev. B **85**, 155310 (2012).

[21] J. D. Mar, J. J. Baumberg, X. Xu, A. C. Irvine, and D. A. Williams, Phys. Rev. B **90**, 241303 (2014).

[22] R. Oulton, J. J. Finley, A. D. Ashmore, I. S. Gregory, D. J. Mowbray, M. S. Skolnick, M. J. Steer, S. L. Liew, M. A. Migliorato, and A. J. Cullis, Phys. Rev. B **66**, 045313 (2002).

[23] T. M. Godden, S. J. Boyle, A. J. Ramsay, A. M. Fox, and M. S. Skolnick, Appl. Phys. Lett. **97**, 061113 (2010).

[24] R. J. Warburton, C. Schäflein, D. Haft, F. Bickel, A. Lorke, K. Karrai, J. M. Garcia, W. Schoenfeld, and P. M. Petroff, Nature (London) **405**, 926 (2000).

[25] H. J. Krenner, S. Stufler, M. Sabathil, E. C. Clark, P. Ester, M. Bichler, G. Abstreiter, J. J. Finley, and A. Zrenner, New J. Phys. **7**, 184 (2005).

[26] A. Zrenner, E. Beham, S. Stufler, F. Findeis, M. Bichler, and G. Abstreiter, Nature (London) **418**, 612 (2002).

[27] S. Stufler, P. Ester, A. Zrenner, and M. Bichler, Phys. Rev. B **72**, 121301 (2005).

[28] K. Müller, A. Bechtold, C. Ruppert, T. Kaldewey, M. Zecherle, J. S. Wildmann, M. Bichler, H. J. Krenner, J. M. Villas-Bôas, G. Abstreiter, M. Betz, and J. J. Finley, Ann. Phys. (Leipzig) **525**, 49 (2013).

[29] K. Müller, A. Bechtold, C. Ruppert, M. Zecherle, G. Reithmaier, M. Bichler, H. J. Krenner, G. Abstreiter, A. W. Holleitner, J. M. Villas-Boas, M. Betz, and J. J. Finley, Phys. Rev. Lett. **108**, 197402 (2012).

[30] See Supplemental Material at http://link.aps.org/supplemental/10.1103/PhysRevB.92.115306. For calculating the PC-amplitude of the $h^+ \rightarrow X_+$ transition we use a rate equation model of the QD-population that incorporates three levels, namely the cgs, X_0 and X_+ as schematically illustrated in

Fig. 1(c). The resulting set of differential equations describing the population dynamics can be solved analytically to obtain a sum of exponentials as a fit function for the PC-amplitude of the $h^+ \to X_+$ transition.

[31] Y. A. Goldberg and N. M. Schmidt, in *Handbook Series on Semi-conductor Parameters*, Vol. 1 (World Scientific, London, 1999), pp. 191–213.

[32] P. W. Fry, J. J. Finley, L. R. Wilson, A. Lemaitre, D. J. Mowbray, M. S. Skolnick, M. Hopkinson, G. Hill, and J. C. Clark, Appl. Phys. Lett. **77**, 4344 (2000).

[33] J. M. Villas-Bôas, S. E. Ulloa, and A. O. Govorov, Phys. Rev. Lett. **94**, 057404 (2005).

[34] A. J. Ramsay, A. V. Gopal, E. M. Gauger, A. Nazir, B. W. Lovett, A. M. Fox, and M. S. Skolnick, Phys. Rev. Lett. **104**, 017402 (2010).

[35] P. L. Ardelt, L. Hanschke, K. A. Fischer, K. Müller, A. Kleinkauf, M. Koller, A. Bechtold, T. Simmet, J. Wierzbowski, H. Riedl, G. Abstreiter, and J. J. Finley, Phys. Rev. B **90**, 241404 (2014).

[36] A. J. Ramsay, T. M. Godden, S. J. Boyle, E. M. Gauger, A. Nazir, B. W. Lovett, A. M. Fox, and M. S. Skolnick, Phys. Rev. Lett. **105**, 177402 (2010).

[37] The lower boundary of the dephasing rate corresponding to the intensity damping of the Rabi oscillations can be calculated to be smaller than $\Gamma_{2,\mathrm{phonons}}^{-1} = K_2(T = 4.2 \text{ K})\Omega_{3\pi} = 35.3$ ps for the maximum Rabi frequency of $\Omega = 3\pi$ and a 5 ps long excitation pulse. We use a typical material dephasing time constant $K_2(T = 4.2 \text{ K}) \cong 0.1$ ps for InGaAs QDs at $T = 4.2$ K [34].

[38] J. R. Johansson, P. D. Nation, and F. Nori, Comput. Phys. Commun. **183**, 1760 (2012).

[39] J. J. Finley, M. Sabathil, P. Vogl, G. Abstreiter, R. Oulton, A. I. Tartakovskii, D. J. Mowbray, M. S. Skolnick, S. L. Liew, A. G. Cullis, and M. Hopkinson, Phys. Rev. B **70**, 201308 (2004).

[40] A. Bechtold, D. Rauch, F. Li, T. Simmet, P.-L. Ardelt, A. Regler, K. Müller, and J. J. Finley, arXiv:1410.4316.

[41] A. J. Brash, L. M. P. P. Martins, F. Liu, J. H. Quilter, A. J. Ramsay, M. S. Skolnick, and A. M. Fox, Phys. Rev. B **92**, 121301 (2015).